ICANS-XIV
14th Meeting of the International Collaboration on
Advanced Neutron Sources
June 14-19, 1998
Argonne National Laboratory, 9700 S. Cass Avenue, Argonne, IL 60439, USA

Measurement of Incident Proton Beam Characteristics for AGS Spallation Target Experiment

H. Nakashima, H. Takada, S. Meigo, Y. Kasugai, Y. Ikeda,
Y. Oyama, N. Watanabe and ASTE collaboration

Center for Neutron Science
Japan Atomic Energy Research Institute
Tokai-mura, Naka-gun, Ibaraki-ken, 319-1195, JAPAN

Abstract

In order to determine the initial conditions of the spallation integral experiments using a mercury target bombarded with high energy protons provided by the Alternating Gradient Synchrotron (AGS) accelerator at Brookhaven National Laboratory (BNL), the profile and the total number of incident protons were measured using an electrical method with multi-wire profile monitor, an imaging plate technique and an activation reaction of $Cu(p,x)^{24}Na$. The total number of incident protons was estimated $(6.61\pm0.74)\times10^{13}$, $(3.57\pm0.40)\times10^{13}$ and $(1.84\pm0.21)\times10^{13}$ at the proton energies of 1.5, 7.0 and 24 GeV, respectively.

1. Introduction

In order to study the neutronic, thermal and mechanical characteristics of a mercury target as a spallation neutron source, a series of integral experiments has been started since 1997 using the short pulse, high energy proton beam of 1.5, 7.0 and 24.0 GeV from the Alternating Gradient Synchrotron (AGS) at Brookhaven National Laboratory (BNL). The profile and the number of incident protons are of interest as giving initial conditions for analyzing neutron flux, temperature distribution and pressure wave induced in the mercury target. From an analytical point of view, it is required to measure the profile with spatial resolution of a few mm.

The first experiment was performed under the following conditions : (1) No beam focusing magnet was installed on the beam line after the last switching magnet at the beam extraction point of AGS in spite that the mercury target was placed about 60 m downstream from the extraction point. Resultantly, it was expected that the horizontal and vertical widths including 95 % of the total beam were about 3 cm and 4.5 cm, respectively. (2) Beam diagnostics devices such as current transformer and secondary emission chamber was not settled in the beam line, though on-line measurement of the proton beam was required for temperature and pressure wave measurements. (3) Beam intensity was expected to be as high as 3.6×10^{12} to 5.7×10^{13} protons per bunch.

Considering the above experimental conditions and requirements, an electrical method using a multi-wire profile monitor (MWPM) and an imaging plate technique which measures the intensity distribution of an activated foil were employed for the beam profile measurement. The former provides us the profile pulse by pulse, though the profile is measured as the integrated charges along a wire. The latter gives us the beam intensity at an optional point of the imaging plate, so that more detailed profile information can be obtained in comparison with MWPM. For obtaining total number of incident protons, the activation method with the $Cu(p,x)^{24}Na$ reaction was used, because the reaction has threshold energy about 400 MeV and its cross sections have been well studied. It is noted that neutrons are emitted back to the activation foil from the mercury target when proton beam is injected on the target. However, the spectrum of the neutrons emitted backward generally have no high energy component. It

Keywords: Multi-wire profile monitor, Imaging plate, $Cu(p,x)^{24}Na$

is necessary, therefore, to select a certain threshold reaction which is insensitive to the neutron at least below a several hundreds of MeV.

2. Experimental Procedure

The set up of MWPM and monitor foils is illustrated in Fig. 1. Proton beam passing through the open air from the duct end of the beam line are incident to the mercury target settled 50 cm downstream of the duct end. The target is a cylinder of the mercury of 20 cm in diameter and 120 cm in length with the front surface of a hemisphere of 10 cm radius encapsulated by the stainless steel of 2.5 mm in thick. The MWPM was placed 44 cm upstream of the inside surface of the mercury target, while the monitor foils were placed 6 cm in front of the mercury target.

The MWPM is composed of 32 Au coated tungsten wires of 20 mm in diameter with intervals of 6 mm in both horizontal and vertical direction with respect to the beam axis. The induced charge by the emission of electrons was amplified wire by wire with an amplifier connected to the MWPM. The amplified signals were integrated by 30 msec interval and then converted its amplitude into proportional digits. The signal integration in the amplifier was triggered by a timing signal provided from the AGS accelerator. Time-integrated data during the irradiation were collected into a personal computer (PC), and each integrated signal for each shot was also taken into the PC as a list-mode data.

Two copper foils of 0.1 mm thickness with an area of 100 x 200 mm^2 were put on an aluminum frame together with a 0.025 mm thick aluminum one so as to cover the area of 200 x 200 mm^2. The purity of copper and aluminum foils was 99.99% and 99.5%, respectively. After irradiation, these foils were removed from the frame and intensity of induced activities in the foils were measured by two kind of techniques as followings.

The aluminum foil was attached on an imaging plate closely for 2 weeks in a low-background room after enough cooling time for short-lived nuclei such a ^{24}Na to decay out. As a result, the imaging plate was exposed by the γ and β rays from ^{22}Na and ^{7}Be. The relative exposure dose in each pixel having the area of 200 μm^2 were read out by an imaging plate reader manufactured by Fuji Film Co. Ltd.

The copper foils were cut to 100 pieces with a cross section of 20 x 20 mm^2. These pieces were stacked by every 10 pieces, and then the induced activity of ^{24}Na was measured by a Ge-detector(CANBERRA GC-5019/S) whose resolution was 1.8 keV for 1332 keV γ-peak and peak compton ratio over 64 in catalog value. The data was acquired by a multi-channel analyzer (CANBERRA Genie PC) with 8k channels. The position at the distance of 5 cm on the axis from the surface of Ge-detector was selected as the standard point for absolute γ-ray intensity measurement. The reaction rate of $Cu(p,x)^{24}Na$, Y_j, in j-th foil stack is obtained by correcting the decay through the irradiation, cooling and measuring period, detector efficiency, sum peak effect in counting and so on.

According to the beam operation data logged by the AGS control, the fluctuation of proton flux was as small as a few percent during irradiation period. Therefore, it is possible to assume that protons were supplied constantly as a function of time. Then, proton flux on j -th foil stack, ϕ_j, is represented as:

$$\phi_j = \frac{N_{p,j}}{S_j \cdot T_r}, \tag{1}$$

where, $N_{p,j}$, S_j and T_r indicate the total number of protons incident on the j -th foil stack, the area of the foil stack and irradiation period, respectively. Since the reaction rate, Y_j, is expressed as:

$$Y_j = N_A \frac{w_j}{M} \cdot \sigma \cdot \phi_j, \tag{2}$$

total incident number of protons is obtained from the above equations:

$$N_p = \sum_{j=1}^{10} \frac{M}{N_A \cdot w_j} \cdot \frac{Y_j}{\sigma} \cdot S_j \cdot T_r, \qquad (3)$$

where M indicates the atomic mass of copper, N_A the Avogadro's number, w_j the weight of j-th foil stack, σ the cross section of $Cu(p,x)^{24}Na$ reaction.

In order to estimate the number of protons injected on the mercury target, the fraction of intensity inside the circle with a diameter of 20 cm to that of whole copper sheet was estimated from the measured values by the imaging plate technique. The fractions for three incident energies of 1.5, 7.0 and 24.0 GeV are summarized in Table 1. The data used to obtain the total incident number of protons were listed in Table 2. The physical constants used in the γ-ray spectrometry were taken from Ref. 1. The detector efficiency was determined by a γ-ray measurement using calibrated radioactive standard sources. The cross sections of the $Cu(p,x)^{24}Na$ reaction at proton energies of 1.5, 7.0 and 24.0 GeV were estimated from the experimental data [2-5]. The measured cross sections of the $Cu(p,x)^{24}Na$ reaction are plotted as a function of proton energy in Fig. 2.

In this measurement, the sources of the error were attributed to the following items.

1) Statistical error of peak count
2) Detector efficiency error
3) Uncertainty of the cross section of $Cu(p,x)^{24}Na$
4) Error of weight of foil stack

The statistical error of peak count was in the range from 1.8% to 5.3%. The detector efficiency error was estimated as 5.0% at 1369 keV. The uncertainty of the cross section of $Cu(p,x)^{24}Na$ was estimated as 10.0% from the recent data [2-5] as shown in Fig. 2. The error of the weight of foil stack was less than 0.1%. The errors concerning to the decay constant, γ-ray branching ratio, irradiation time, measuring time, cooling time were negligible in the present work.

3. Results and Discussion

3.1 Beam Profile

The two-dimensional plots of beam profile measured by the imaging plate method are shown in Figs. 3 to 5 for the incident proton energies of 1.5, 7.0 and 24.0 GeV. It is note that these data are obtained by the integration in area of 2 mm x 2 mm for getting enough counting statistics. The projections to horizontal and vertical axes are shown in Figs. 6 and 7 for the proton energies of 1.5 and 24 GeV, respectively. It is observed that the beam profile differ from each other very much dependent upon incident energy and the beam center is not on the target center.

In Figs. 8 and 9, the integrated values along horizontal and vertical axes obtained by the imaging plate technique are compared with those measured with MWPM for 7.0 GeV proton incidence. It is observed that the results of imaging plate give almost the same full width half maximum (FWHM) as those of MWPM in both directions but the former is somewhat broader than the later. The reason of the broadening may be caused by the resolution of the imaging plate technique. It was found the effective spatial resolution of the profile measured by the imaging plate was estimated to be 3 mm from the measurement at the edge of the aluminum plate.

Since the aluminum foil was placed near the mercury target, it is possible that the foil is activated by the secondary particles emitted backward from the target. An analytical study was also performed to estimate the contribution of the secondary particles to the nuclide production in the aluminum foil. Figure 10 shows the secondary neutron energy spectra calculated by the HERMES code system [6] at the foil position where the measured beam profile was used as the input conditions. The reaction rates of $^{27}Al(p/n,x)^{22}Na$ were calculated using the cross section data evaluated by the ALICE-F code [7], while those of $^{27}Al(p/n,x)^{7}Be$ were obtained from the measured cross sections with protons [8-11], because the cross sections are not calculated by the ALICE-F code and neutron cross section is not measured. These reactions have the threshold energies of about 30 MeV. The calculated results are compared in Tables 3(a) and 3(b) with the measured data by means of γ -ray spectrometry.

It is found in these tables that the HERMES calculation gives 60% lower reaction rates

than the measured data for 1.5 GeV proton incidence, although the calculation includes the contribution of secondary particles. This indicates that ^{22}Na and ^{7}Be have been produced by the forward-scattered particles other than by the incident protons. The forward-scattered particles are seemed to be produced on the structure such as a beam tube. In fact, beam loss of about 30% has been observed in the beam intensity measurement using copper foil as described in the following sub-section. Though it is difficult to estimate the spatial distribution of the forward scattered particles, the distribution is assumed to be almost uniform. Thus, it is seemed that these particles do not distort the relative beam profile. For 7.0 GeV proton incidence, the calculated reaction rates agree with the measured ones within about 10%. According to the calculation, the backward-emitted neutrons produce ^{22}Na about 30% to the total amount, while they produce ^{7}Be only 3%. However, the contribution of the backward-emitted neutrons reduces from 30% to some extent because the activity of ^{7}Be was higher than that of ^{22}Na by a factor of 2 at the exposure period in the imaging plate measurement. For 24.0 GeV proton incidence, it is suggested that about half of ^{22}Na and 20% of ^{7}Be was produced in the aluminum foil by the backward-emitted neutrons. In the additional calculation it was found that the effect of the backward-emitted neutrons can be reduced to less than 10 % for 24 GeV by placing the aluminum foil to 50 cm upstream from the mercury target.

3.2 Total Number of Incident Protons

According to the procedure described in the previous section, the total number of protons was obtained as $(6.61 \pm 0.74) \times 10^{13}$, $(3.57 \pm 0.40) \times 10^{13}$ and $(1.84 \pm 0.21) \times 10^{13}$ for 1.5, 7.0 and 24.0 GeV proton incidence, respectively. In Table 4, these values are compared with those measured with a secondary emission chamber (SEC) and a current transformer (CT) installed in the AGS ring at 50 m upstream of the mercury target.

It is clear that total numbers of incident protons obtained at the secondary container surface are smaller than those measured at 50 m upstream except for 24 GeV proton incidence. This is due to the condition that any focusing magnet was not installed on the beam line, resulting that proton beam diverges and be lost after passing through the last focusing magnet. Furthermore, the arrangement of the magnets in the AGS ring is not well-designed for 1.5 GeV, although the beam profile at the target position is decided by the beam emittance at the extraction magnet under this condition. Therefore, the ratio of total number of incident protons measured by Cu-foil to that of CT becomes the lowest at 1.5 GeV among the three incident energies.

4. Concluding Remarks

In the AGS experiment using the mercury target, the profile and total number of incident protons were measured by using the MWPM, the imaging plate and the activation technique.

The relative beam profiles were obtained for 1.5 7.0 and 24.0 GeV protons using imaging plate technique. The FWHM obtained by the imaging plate technique was somewhat broader than that by MWPM in the beam profile integrated along horizontal and vertical axes. It seems that the data include the uncertainty of several tens of percent because neutrons emitted backward from the mercury target produced ^{22}Na and ^{7}Be in the aluminum foil. The uncertainty increases with increasing the incident proton energy, because of the contribution of backward-emitted neutrons. Since the contribution is as a function of the distance between the foil position and the target, it is necessary to optimize the foil position in the future experiment to improve the quality of data.

The total number of incident protons was measured by the activation reaction of $Cu(p,x)^{24}Na$. The resultant total number of incident protons was estimated as $(6.61 \pm 0.74) \times 10^{13}$, $(3.57 \pm 0.40) \times 10^{13}$ and $(1.84 \pm 0.21) \times 10^{13}$ for 1.5, 7.0 and 24.0 proton incidence, respectively. In comparison with the values measured with the secondary emission chamber and the current transformer in the AGS ring, the values measured by the activation technique were smaller by 73% to 95% than those obtained by the devices in the AGS ring because of lack of beam focusing magnets between the AGS ring and the target.

Acknowledgments

This work has been carried out in a frame of the ASTE collaboration. The authors would like to thank to all the staffs of BNL involved in the ASTE experiment for their help and support. The authors also thank to Prof. Y.Irie and Drs. Y.Yano and S.Muto of KEK for their valuable discussion about beam profile measurement.

References

(1) Lederer, C. M. and Shirley, V. S. (Ed.): "Table of Isotopes 7th Edition", Willey Interscience Publication, N.Y., (1978).
(2) Schopper H. (Ed.): "LANDORT-BÖRNSTEIN, Numerical Data and Functional Relation ships in Science and Technology, New Series, Group I: Nuclear and Particle Physics, Vol. 13, Production of Radionuclides at Intermediate Energies, Subvol. a, Interactions of Protons with Targets from He to Br", Springer-Verlag, Berlin Heidelberg, (1991).
(3) Schopper H. (Ed.): ibid., "subvol. d, Interactions of Protons with Nuclei (Supplement to I/13a. b, c)", Springer-Verlag, Berlin Heidelberg, (1994).
(4) Michel, R., et al.: Nucl. Instrm. Methods, B113, 183 (1995).
(5) Titarenko, Yu. E., et al.: "Experimental and Computer Simulation Study of Radionuclide Yields in the ADT Materials Irradiated with Intermediate Energy Protons", Proc. of 3rd Specialists' Mtg. on High Energy Nucl. Data, Mar. 30-31, 1998, JAERI, Tokai, JAERI-Conf, (to be published).
(6) Cloth, P., et al.: "HERMES A Monte Carlo Program System for Beam Materials Interaction Studies", Jül-2203, (1988).
(7) Fukahori, T.: "ALICE-F Calculation of Nuclear Data up to 1 GeV", Proc. of the Specialists' Mtg. on High Energy Nucl. Data, Oct. 3-4, 1991, JAERI, Tokai, JAERI-M 92-039, pp. 114-122 (1992).
(8) Cumming, J. B., et al.: Phys. Rev., **128**, 2392 (1962).
(9) Furukawa, M., et al.: Nucl., Phys., **69**, 362 (1965).
(10) Bogatin, V. I., et al.: Nucl. Phys, A, **260**, 446 (1976).
(11) Aleksandrov, V. N., et al.: At. Energi, **64**, 445 (1988).

Table 1. Fraction of intensity inside the circle of 20 cm diameter in the copper sheet

Proton Energy	Fraction
1.5 GeV	96 %
7.0 GeV	97 %
24.0 GeV	97 %

Table 2. Data used for obtaining the total incident number of protons

Item	Value
Avogadro's number	6.02×10^{23}
Atomic mass of copper	63.5
Cross section of $Cu(p,x)^{24}Na$	2.00 mb at 1.5 GeV 3.60 mb at 7.0 GeV 3.50 mb at 24.0 GeV
Decay Constant of ^{24}Na	1.29×10^{-5}
γ-ray energy of ^{24}Na	1368.9 keV
Detector efficiency at 5 cm	0.62 % at 1368.9 keV
Branching of 1368.9 keV γ-ray	100%

Table 3 (a). Measured and Calculated ^{22}Na production reaction rates in Al foil

Energy (GeV)	^{22}Na production in ^{27}Al ($x10^{-24}$/proton) Measurement	Calculation	Backward-Emitted Neutron Component in Calculation	Backward-Emitted Proton Component in Calculation	C/E
1.5	$1.79x10^{-2}$	$9.85x10^{-3}$	4%	0.4%	0.55
7.0	$1.50x10^{-2}$	$1.34x10^{-2}$	27%	2.6%	0.89
24.0	$1.61x10^{-2}$	$2.31x10^{-2}$	48%	9.5%	1.43

Table 3 (b). Measured and Calculated ^{7}Be production reaction rates in Al foil.

Energy (GeV)	^{7}Be production in ^{27}Al ($x10^{-24}$/proton) Measurement	Calculation	Backward-Emitted Neutron Component in Calculation	Backward-Emitted Proton Component in Calculation	C/E
1.5	$1.41x10^{-2}$	$8.52x10^{-3}$	2%	< 0.1%	0.60
7.0	$1.01x10^{-2}$	$8.91x10^{-3}$	3%	0.4%	0.88
24.0	$7.11x10^{-2}$	$1.03x10^{-2}$	19%	4.8%	1.45

Table 4. Comparison of total number of incident protons measured by different instruments.

Proton Energy (GeV)	Cu-foil ($x10^{13}$ protons)	S.E.C. ($x10^{13}$ protons)	C.T. ($x10^{13}$ protons)	Ratio of Cu-foil to C.T.
1.5	6.61±0.74	10.8	9.09	0.727
7.0	3.57±0.40	4.20	3.89	0.918
24.0	1.84±0.21	1.83	1.93	0.953

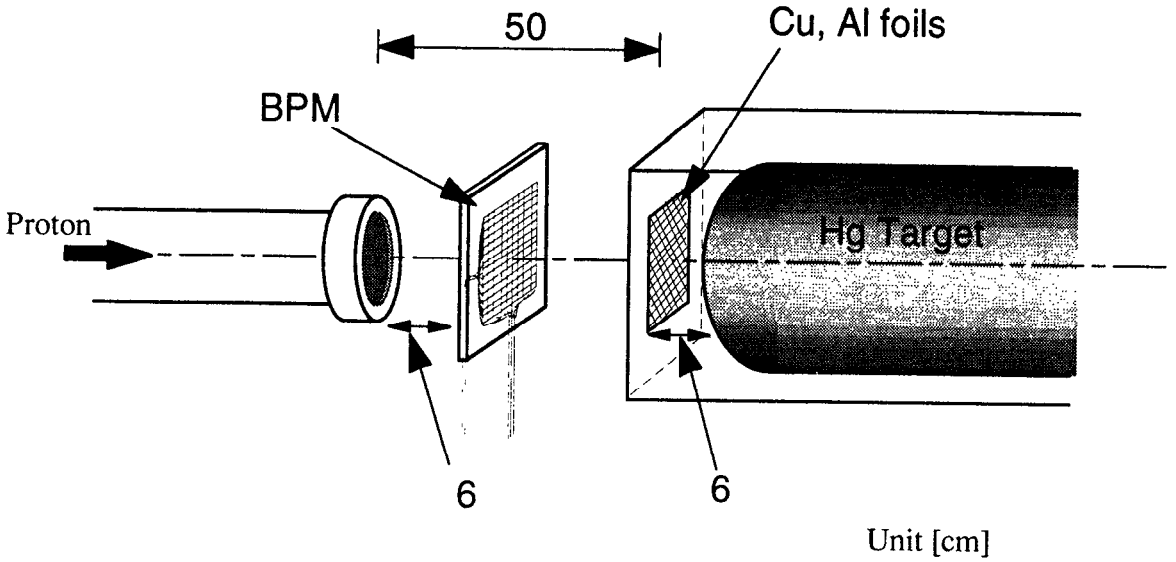

Fig.1 Experimental set up of a beam profile monitors and activation foils.

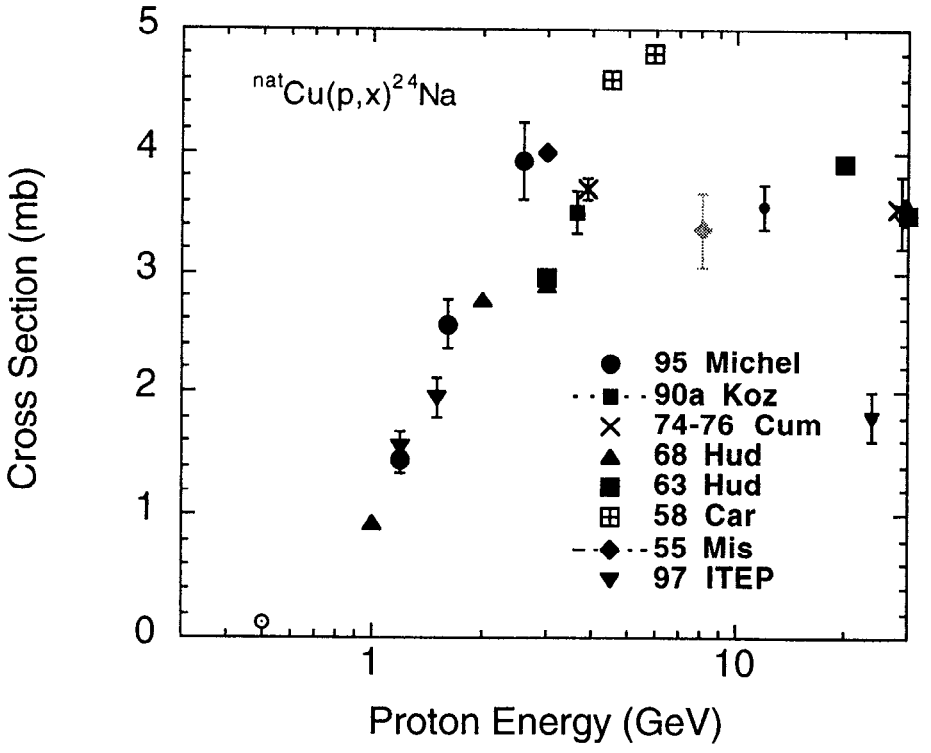

Fig. 2 Experimental neutron cross sections[2-5] of the Cu(n, x)^{24}Na reaction.

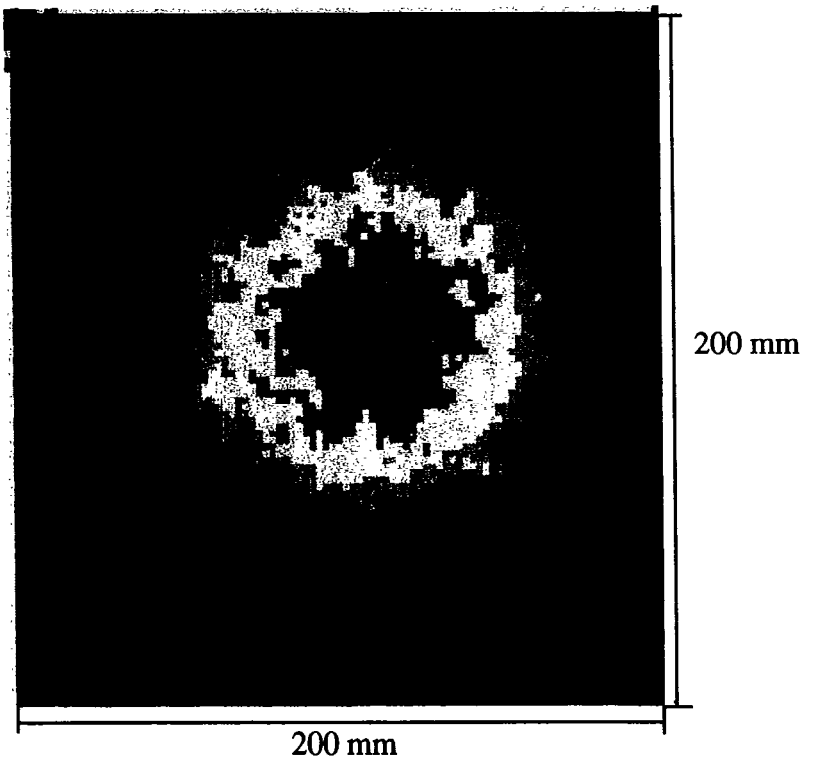

Fig. 3 Two-dimensional plots of beam profile measured with the imaging plate technique for 1.5 GeV proton incidence. The proton beam penetrates from the front surface of the foil to the back.

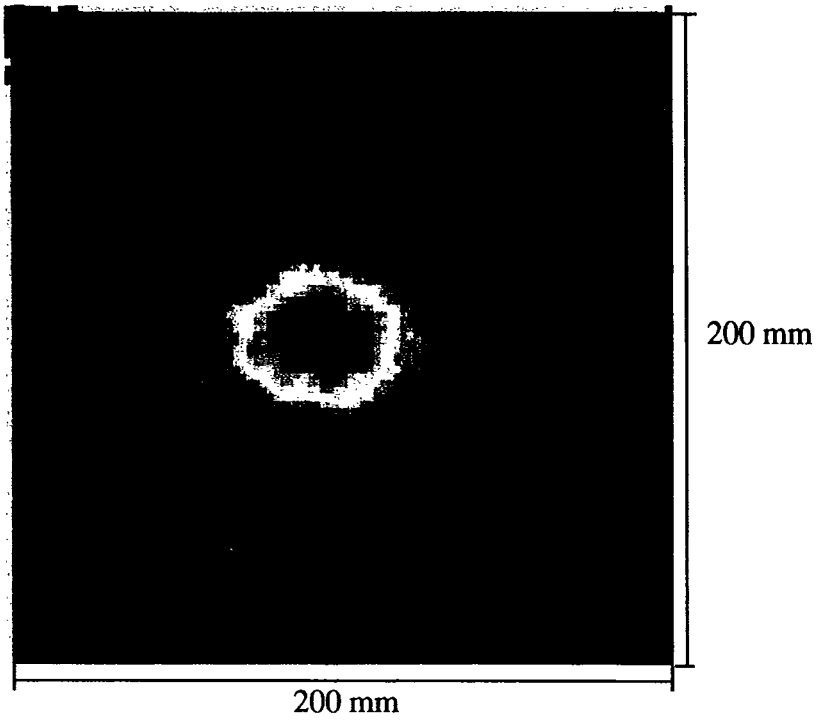

Fig. 4 Two-dimensional plots of beam profile measured with the imaging plate technique for 7.0 GeV proton incidence. The proton beam penetrates from the front surface of the foil to the back.

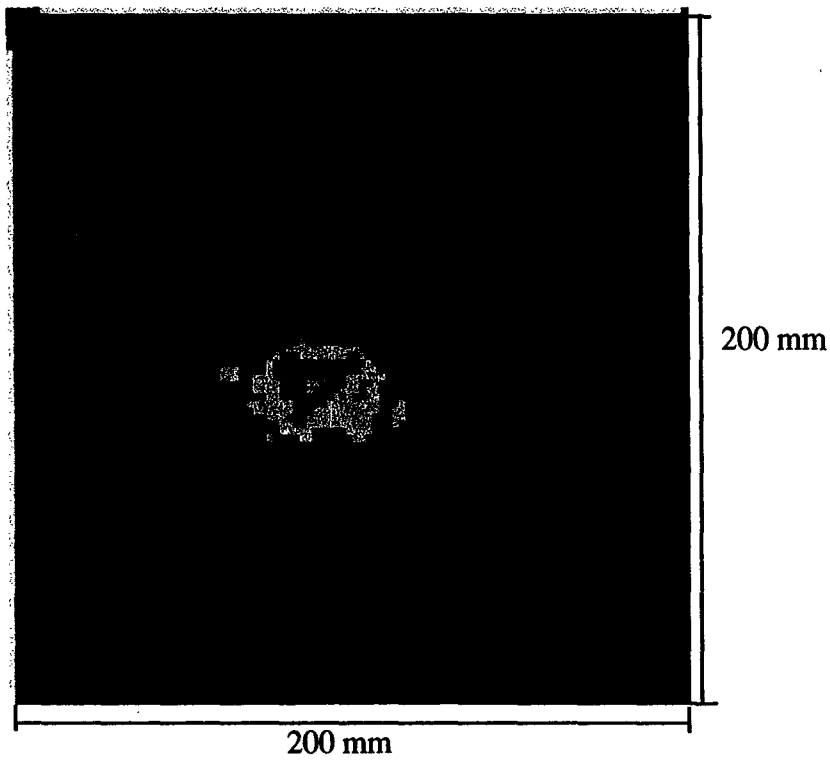

Fig. 5 Two-dimensional plots of beam profile measured with the imaging plate technique for 24.0 GeV proton incidence. The proton beam penetrated from the front surface of the foil to the back.

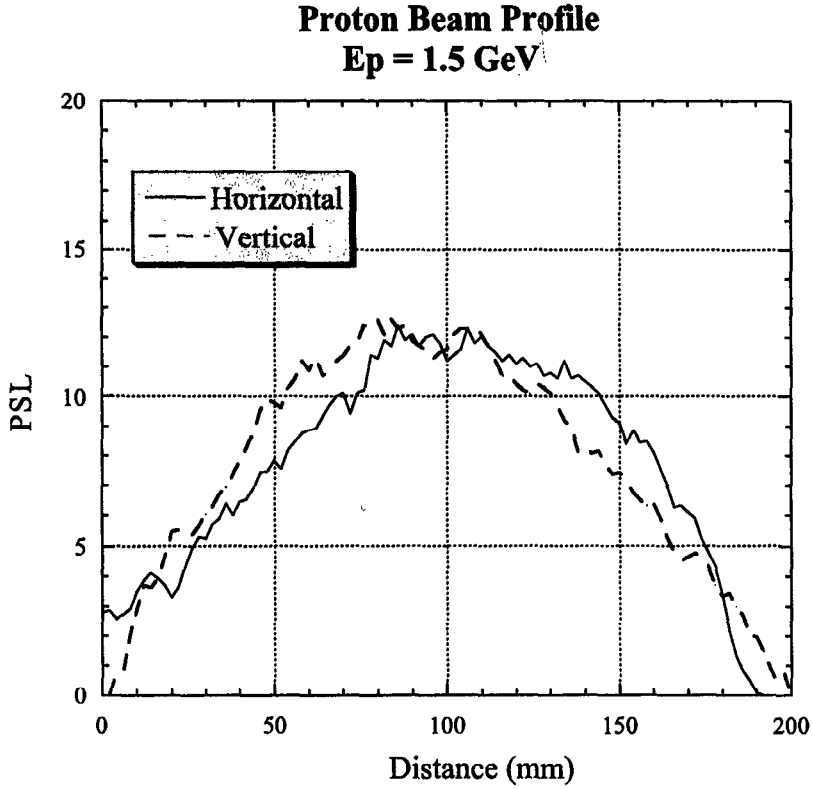

Fig. 6 Projection of beam profiles measured with the the imaging plate technique to horizontal and vertical axes for 1.5 GeV proton incidence.

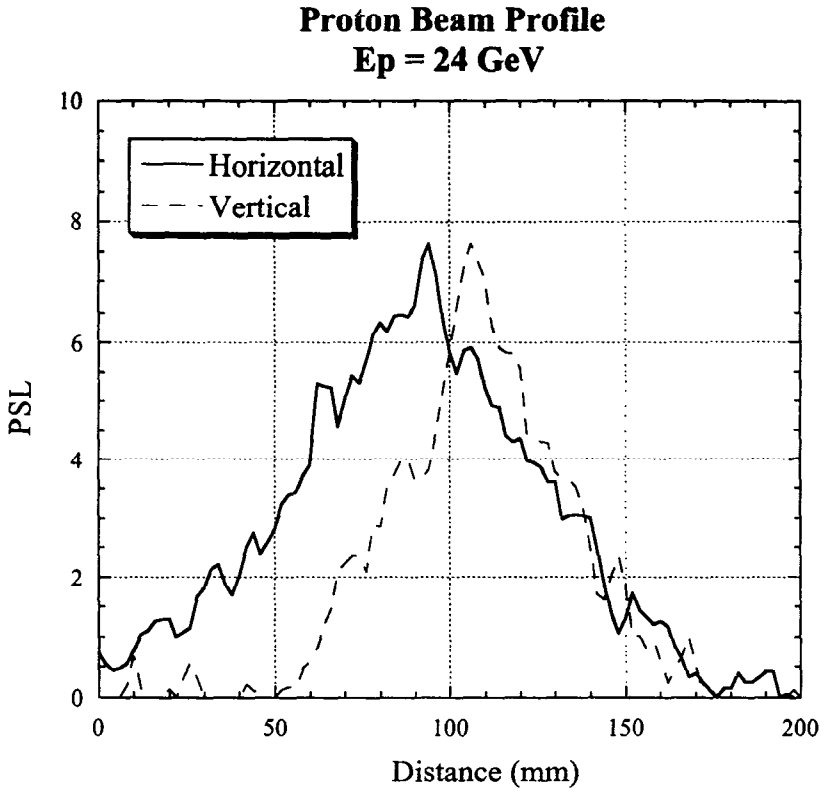

Fig. 7 Projection of beam profiles measured with the imaging plate technique to horizontal and vertical axes for 24.0 GeV proton incidence.

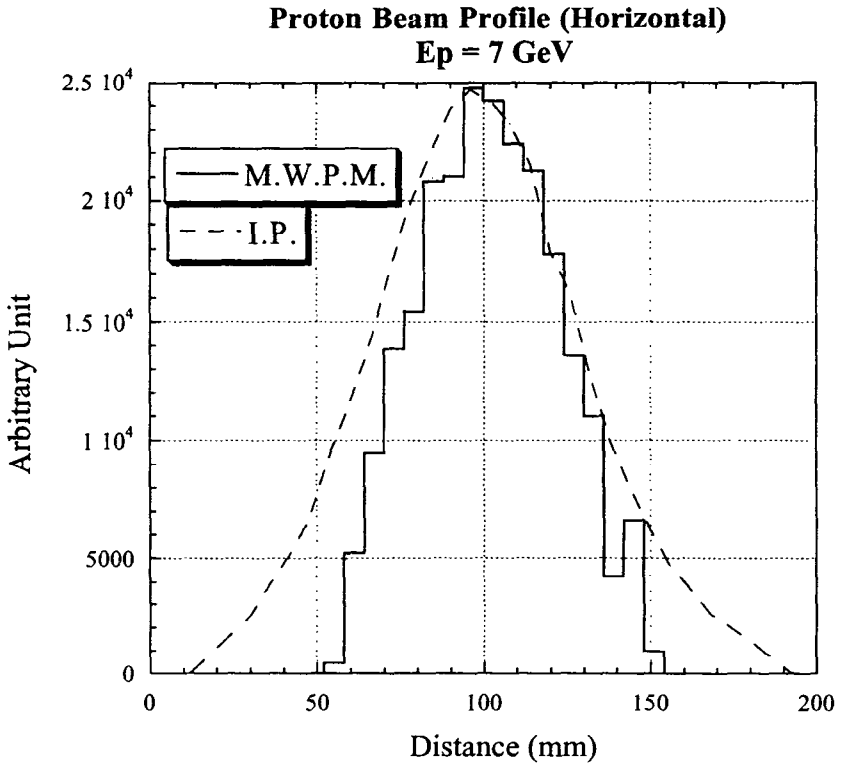

Fig. 8 Comparison of beam profile measured by the imaging plate technique with that obtained by MWPM for 7.0 GeV proton incidence. The profiles are integrated along the vertical axes at each position on horizontal axis.

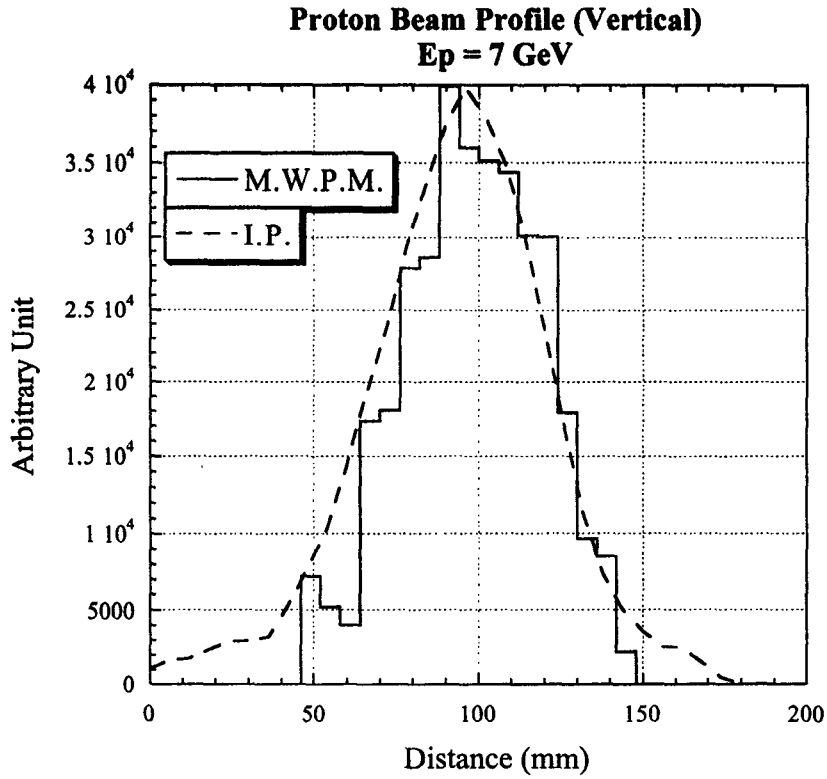

Fig. 9 Comparison of beam profile measured by the imaging plate technique with that obtained by MWPM for 7.0 GeV proton incidence. The profiles are integrated along the horizontal axes at each position on vertical axis.

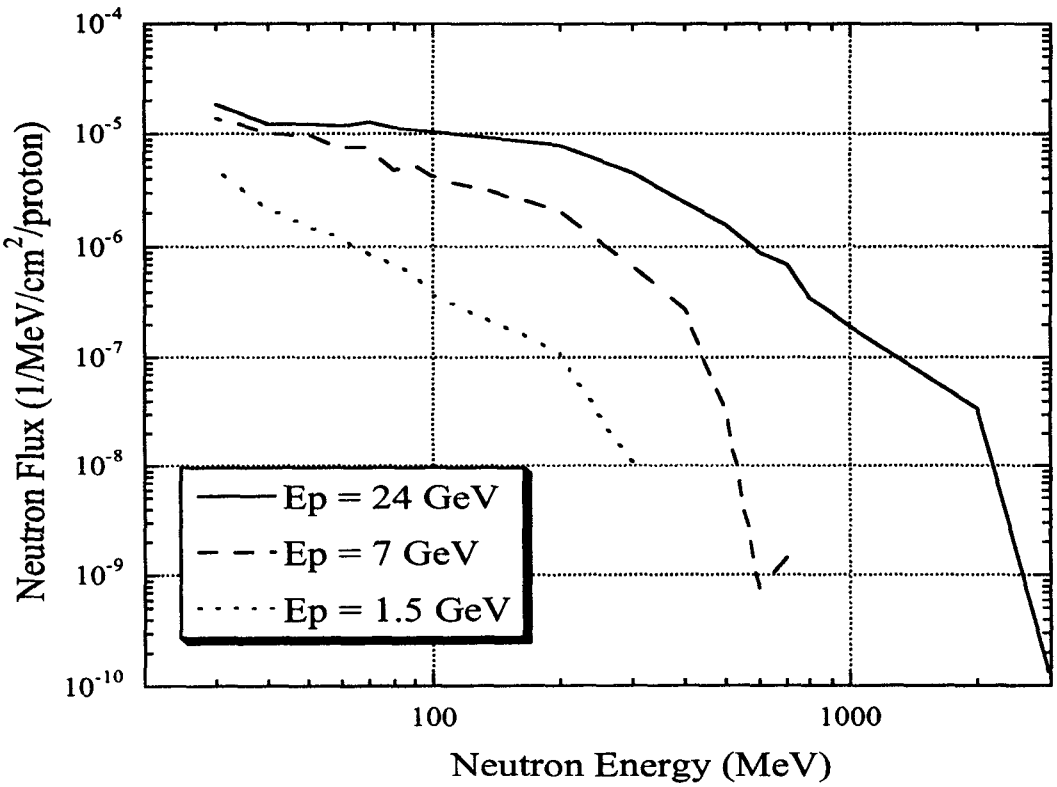

Fig. 10 Neutron fluxes emitted backward from the mercury target at the position where the aluminum foil was placed for 1.5, 7.0 and 24.0 GeV proton incidence. The fluxes were calculated by the HERMES code sysem.